Astrophysics and Space Science (2023) 368:35
https://doi.org/10.1007/s10509-023-04182-6

RESEARCH

Nonlinear electrostatic structures and stopbands in a three-component magnetosheath plasma

O.R. Rufai[1,2] · S.V. Singh[3] · G.S. Lakhina[3]

Received: 8 August 2022 / Accepted: 18 March 2023 / Published online: 25 April 2023

Abstract

Large amplitude parallel propagating electric field structures of nonlinear electron-acoustic waves are examined in an unmagnetized magnetosheath plasma. Based on the observations and simulations by Ergun et al. (2016), the plasma in the magnetosheath side of the ion diffusion layer is modeled by a 3-component adiabatic fluid dynamic plasma consisting of cold magnetospheric (MSP) electrons, magnetosheath electrons, and background ions. Using the Sagdeev pseudopotential technique, for the plasma parameters recorded by the Magnetospheric Multiscale (MMS) mission in the magnetosheath side of the ion diffusion region, existence regime of the nonlinear electrostatic solitary wave structures is obtained with the possibilities of stopbands (forbidden gap region). Stopbands or the forbidden gap region exists even when the drift velocity of the cold electron beam is zero. The forbidden gap region becomes wider and the Mach numbers of the regions supporting solitary structures become larger by an increase in the drift velocity of the cold electron beam. The results are in agreement with the magnetosheath electrostatic waves having amplitudes of 100s mV/m and frequencies up to 3.2 kHz observed by the MMS.

1 Introduction

The Earth's magnetosheath is a region between the magnetopause and the bow shock. This region is predominantly occupied by high plasma fluctuations and turbulence due to several acceleration mechanisms, such as magnetic reconnection (Hui et al. 2020; Huang 2022). Magnetospheric Multiscale (MMS) mission has shown that the broadband electrostatic solitary waves (ESWs) are the consequence of symmetric and asymmetric magnetic reconnection processes in the diffusion region of the Earth's magnetopause (Ergun et al. 2016; Graham et al. 2018; Argall et al. 2018) and the magnetotail (Lotekar et al. 2020; Dillard et al. 2018; Vasko et al. 2017; Kamaletdinov et al. 2021). In general, electrostatic solitary waves (ESWs) are the most common interpretations for the plasma turbulence and fluctuations observed in different regions of the Earth's magnetosphere such as auroral region (Temerin et al. 1982; Bostrom et al. 1989; Ergun et al. 1998), polar cup boundary layer (Tsurutani et al. 1998), plasma sheet boundary layer (Matsumoto et al. 1994; Tong et al. 2018), magnetosheath (Pickett et al. 2003, 2004, 2005), magnetopause (Graham et al. 2015), Earth's radiation belts (Mozer et al. 2015; Vasko et al. 2018; Lotekar et al. 2019), and the solar wind and Earth's bow shock (Goodrich et al. 2018; Vasko et al. 2020; Mozer et al. 2021; Wang et al. 2021).

A large number of theoretical approaches to study the ESWs have been done. Apart from the Bernstein-Greene-Kruskal (BGK) mode of kinetic electron/ion phase space holes (Bernstein et al. 1957; Schamel 1972; Omura et al. 1994; Muschietti et al. 1999; Hutchinson 2017), the fluid dynamics approach (Berthomier et al. 1998; Kakad et al. 2007; Lakhina et al. 2009, 2011a,b, 2018, 2021; Maharaj et al. 2012a,b; Rubia et al. 2016a,b; Rufai et al. 2012, 2014; Rufai 2015; Rufai and Bharuthram 2016, 2019; Bharuthram et al. 2022; Singh et al. 2011) has been helpful and widely used to study the nonlinear electrostatic solitary waves (ESWs) phenomena in space plasmas. This fluid approach gives a

✉ O.R. Rufai
odutayoraji.rufai@nasa.gov

S.V. Singh
satyavir@iigs.iigm.res.in

G.S. Lakhina
lakhina@iigs.iigm.res.in

1 Heliophysics Division, NASA Goddard Space Flight Center, Greenbelt, MD, USA

2 Department of Physics, Catholic University of America, Washington DC, USA

3 Indian Institute of Geomagnetism, New Panvel (W), Navi Mumbai 410218, India

simple physical assessment and interpretation of the broadband plasma wave spectrum. In this case, each plasma component is treated as mobile species by using the set of equations, such as, continuity equation, momentum equation and equation of state. In a four-component plasma, Lakhina et al. (2008) predicted the possibilities of having three types of solitary structures, namely, slow ion-acoustic, ion-acoustic and electron-acoustic solitons depending on the Mach number values. The large-amplitude multi-fluid plasma model considered has cold background electrons and ions, a hot electron beam and a hot ion beam. In a later paper, Lakhina et al. (2011a) predicted another three sets of solitary waves named by ion-acoustic, slow and fast electron-acoustic soliton/double layer in a multi-component unmagnetized plasma consisting of background electrons, counter-streaming electron beams and ions. Exploiting the Cluster spacecraft data in the Earth's northern plasma sheet boundary layer (PSBL) region, Kakad et al. (2016) revealed the co-existence of slow and fast ion-acoustic waves and electron-acoustic waves in a four-component multi-fluid model consisting of a cold electron, hot electron, cold proton, and hot proton species, respectively. Using the reductive perturbation technique which leads to a modified Korteweg-de Vries (mKdV) equation of small but finite amplitude electrostatic structures, Rufai et al. (2021a) studied the existence of nonlinear high-frequency electron-acoustic solitons in the electron diffusion region. They considered a plasma model composed of a hot trapped electrons having vortex-like velocity distribution and a warm fluid adiabatic electrons. The model is later extended by Rufai et al. (2022) to include a cold electron beam to investigate large-amplitude parallel electric field structures in the diffusion region of the Earth's magnetopause, using the Sagdeev pseudopotential technique. They predicted the possibilities of slow electron-acoustic and beam modes as the consequences of the asymmetry magnetic reconnection in the ion diffusion region of the Earth's magnetopause observed by the MMS satellite.

In space and astrophysical plasmas, singularities can be observed in the broadband plasma wave phenomena due to wave discontinuities or breaks in the linear or nonlinear dispersion properties (Bulanov et al. 2012a,b). Physically, singularities may appear as surges or stopbands with respect to some continuous physical parameters, such as, density, pressure, temperature, velocity, electric field, etc. These could be observed during the magnetic reconnection process in the magnetosphere. Using THEMIS parameters, Rufai et al. (2021b) revealed the possibilities of wave singularities associated with the Sagdeev potential structures in a four-component suprathermal plasma consisting of a fluid cold singly-charged oxygen ions, hot protons, and two distinct groups of electrons with the latter three having kappa velocity distributions for an obliquely propagation low-frequency electrostatic fluctuations in the magnetopause and plasma sheet regions of the Earth's magnetosphere. The coexistence of electrostatic compressive (positive potential) and rarefactive (negative potential) solitons limited by a double layer formation as the upper band limit of the nonlinear structures have been presented by Rufai et al. (2016), for the auroral region plasma parameters observed by Viking satellite. For the lunar wake plasma parameters, Rubia et al. (2018) studied nonlinear solitary waves and double layer in a four-component plasma consisting of hot protons, hot heavier ions (He^{++}), electron beam, and suprathermal (κ-distribution) electrons. They showed that both slow and fast ion-acoustic modes support a "forbidden gap", the region in which the soliton ceases to propagate. The stopbands region in nonlinear fast ion-acoustic soliton structures in multi-component plasmas have been discussed by Maharaj and Bharuthram (2020) and, later by Verheest and Hellberg (2020).

In our previous paper (Rufai et al. 2022), we study the large-amplitude electrostatic solitary waves (ESWs) during the magnetosphere and magnetosheath events of the ion diffusion region at the Earth's magnetopause for the parameters used in the simulation of electron-acoustic mode by Ergun et al. (2016). Moreover, in the absence of hot electron species, the Vlasov simulation presented from the data set in Fig. 3(f) of Ergun et al. (2016) depicted the possibilities of the electrostatic solitary waves with two electron distributions (cold MSP and warm magnetosheath electrons) in the magnetosheath side of the ion diffusion region. This event is best described by a beam mode (Ergun et al. 2016). In the magnetosheath side, Rufai et al. (2022) obtained positive potential soliton structures only corresponding to a low value of the cold electron number density ($n_{c0} = 0.007$) and higher drift velocity ($v_{dc} = 101$). Here, we further our investigation on the large-amplitude ESWs during the magnetosheath event of the ion diffusion region (Ergun et al. 2016) by undertaking a detailed analysis of the existence domain as well as the characteristics of the electron-acoustic solitons (beam mode) over a broad parametric range of cold electron densities and their drift velocities. Not only we find existence of negative solitons and double layers in the magnetosheath, but we also discover the phenomenon of a stopband or forbidden gap where no solitons/double layers can propagate. In Sect. 2, the plasma model and derivation of the Sagdeev pseudopotential for the localized nonlinear structures are presented. The numerical results are presented in Sect. 3. Lastly, the discussion and conclusion of the findings are given in Sect. 4.

2 Theoretical model

The present plasma model is guided by the energetic particle distributions observed during the magnetosheath event of the ion diffusion layer, generating beam instability recorded by Ergun et al. (2016) (cf. Fig. 3(f)) from the MMS observations. These large-amplitude broadband electrostatic solitary waves recorded in the magnetosheath side appear to be primarily driven by two-electron populations. Based on these observations, we consider propagation of large-amplitude high-frequency waves in a three-component, homogeneous, collisionless and unmagnetized plasma system composed of a cold magnetospheric (MSP) electrons (N_c, T_c, V_{dc}) propagating parallel to the magnetic field with respect to the warm magnetosheath electrons (N_w, T_w, V_{dw}) drifting antiparallel, and background ions (N_i, T_i). Where the notations, N_j, T_j, V_{dj} represents the equilibrium values of density, temperature and drift velocity of the species j, and $j = c, w$ and i for the cold, warm electrons, and ions, respectively. The magnetosheath plasma model are governed by the following adiabatic fluid equations (i.e., continuity, momentum, equation of state, and Poisson equation, respectively) (Lakhina et al. 2009; Rufai et al. 2022):

$$\frac{\partial n_j}{\partial t} + \frac{\partial (n_j v_j)}{\partial x} = 0, \tag{1}$$

$$\frac{\partial v_j}{\partial t} + v_j \frac{\partial v_j}{\partial x} + \frac{1}{\mu_j n_j}\frac{\partial P_j}{\partial x} + \frac{Z_j}{\mu_j}\frac{\partial \phi}{\partial x} = 0, \tag{2}$$

$$\frac{\partial P_j}{\partial t} + v_j \frac{\partial P_j}{\partial x} + 3P_j \frac{\partial v_j}{\partial x} = 0, \tag{3}$$

$$\frac{\partial^2 \phi}{\partial x^2} = -\sum_j Z_j n_j. \tag{4}$$

Here, n_j, v_j, P_j, and $\mu_j = m_j/m_i$, density, velocity, pressure, and mass ratio of the jth species and the ions, $Z_j (= -1(+1))$ for electrons (ions), respectively. The number densities are normalized by the total equilibrium plasma density $n_{j0} = N_j/N_0$ such that $n_{c0} + n_{w0} = n_{i0} = 1$. The normalizations used are as follows, the temperatures are normalized by the ion temperature T_i, time is normalized by the inverse of ion plasma frequency, $\omega_{pi}^{-1} = (4\pi N_0 e^2/m_i)^{-1/2}$, velocities by the ion thermal velocity $v_{ti} = (T_i/m_i)^{1/2}$, spatial lengths by $\lambda_{di} = (T_i/4\pi N_0 e^2)^{1/2}$, electrostatic potential ϕ is normalized by T_i/e, and the thermal pressures P_j by $N_0 T_i$. The adiabatic index $\gamma = 3$ (for the case of a 1-D system) is justified for all the mobile species (e.g. cold, warm electrons and ions) in the equation of state given by equation (3).

Analytically, we employ the Sagdeev pseudo-potential technique (Sagdeev 1966) to derive the energy integral equation (which conserve the full complexity of the localized nonlinear structures) for the large amplitude electrostatic solitary waves. The derivation involved the transformation of all the dependent variables in equations (1)-(4) to a single independent variable in a moving frame of reference (Rufai et al. 2022), i.e. $\xi = x - Mt$, where $M = V/v_{ti}$ (V is the wave phase speed – in the frame of background ions).

Then, solving for the perturbed densities of cold, warm electrons and ions in equations (1)-(3) above and substituting these expressions into the Poisson equation (4), and assuming appropriate boundary conditions for the nonlinear localized structures such as, $n_j \to n_{j0}$, $v_j \to v_{dj}$, $\phi = d\phi/d\xi \to 0$, and $P_j \to P_{j0} \sim n_{j0}T_j/T_i$ at $\xi \to \pm\infty$, we obtain the following energy integral (Schamel 1979; Singh et al. 2001)

$$\frac{1}{2}\left(\frac{d\phi}{d\xi}\right)^2 + S(\phi, M) = 0, \tag{5}$$

where the Sagdeev potential $S(\phi, M)$ is written as (Kakad et al. 2016; Rufai et al. 2022)

$$\begin{aligned} S(\phi, M) = \sum_j \frac{n_{j0}\mu_j}{6\sqrt{3\delta_j}} \Bigg[\Bigg[&\left((M - v_{dj}) + \sqrt{3\delta_j}\right)^3 \\ &- \left(\sqrt{\left((M - v_{dj}) + \sqrt{3\delta_j}\right)^2 - \frac{2Z_j\phi}{\mu_j}}\right)^3 \Bigg] \\ &\pm \Bigg[\left((M - v_{dj}) - \sqrt{3\delta_j}\right)^3 \\ &- \left(\sqrt{\left((M - v_{dj}) - \sqrt{3\delta_j}\right)^2 - \frac{2Z_j\phi}{\mu_j}}\right)^3 \Bigg]\Bigg], \end{aligned} \tag{6}$$

where $\delta_j = \frac{P_{j0}}{n_{j0}\mu_j}$. Equation (5) describes the motion of a pseudo-particle of unit mass in a Sagdeev pseudo-potential $S(\phi, M)$ where ϕ and ξ are the displacement from the equilibrium and time, respectively.

The energy integral (5) and the Sagdeev potential $S(\phi, M)$ presented in equation (6) constitute the basic equations for the analysis of the arbitrary large-amplitude electrostatic solitary waves (ESWs) through the Sagdeev pseudo-potential technique (Sagdeev 1966). The criteria for solitary wave solutions are: the Sagdeev potential $S(\phi, M)$ must satisfies the following conditions: $S(\phi, M) = 0$, $dS(\phi, M)/d\phi = 0$, and $d^2S(\phi, M)/d\phi^2 < 0$ at $\phi = 0$; $S(\phi, M) = 0$ at $\phi = \phi_m$ and $S(\phi, M) < 0$ for $0 < |\phi| < |\phi_m|$, where ϕ_m is the maximum potential. For double layer (DL) solutions, one more additional condition should be satisfied, namely, $dS(\phi, M)/d\phi = 0$ at $\phi = \phi_m$ (Lakhina et al. 2009).

The Sagdeev potential $S(\phi, M)$ and its first derivative with respect to ϕ vanish at $\phi = 0$. For the Mach number domain, the condition $d^2S(\phi, M)/d\phi^2 < 0$ at $\phi = 0$ is satisfied provided $M > M_0$, where the critical Mach number M_0 satisfies the following equation, i.e.,

$$\frac{d^2S(\phi, M)}{d\phi^2}\Big|_{\phi=0} = f(M_0)$$

$$\equiv \sum_j \frac{n_{j0}}{\mu_j\left((M_0 - v_{dj})^2 - 3\delta_j\right)} = 0. \tag{7}$$

Solving equation (7) numerically, it yields 4 roots as the critical Mach numbers (M_0) but only two are positive roots with physical interpretations, which correspond to the two nonlinear modes, namely, ion-acoustic mode and electron-acoustic (beam) mode. Unlike, the case of four-component plasma populations (cold magnetospheric (MSP) electrons, warm magnetosheath electrons, a vortex-like hot electrons, and background ions) studied earlier by Rufai et al. (2022) which can yields up to 6 roots as the critical Mach number. In that case, only 3 are positive roots which correspond to the physical interpretation of three nonlinear modes of ion-acoustic, slow electron-acoustic and fast electron-acoustic modes. Moreover, it has been well established (Lakhina et al. 2008, 2009, 2011a) that for a given set of plasma parameters, any one, or both modes can satisfy the nonlinear electrostatic solitary wave conditions given above. From Eq. (7), it is seen that when the denominator of any of the species becomes close to 0, it produces singularity and there is no solution for critical Mach numbers. This condition leads to the existence of stopbands or forbidden gaps. Furthermore, when for a given parametric range, the roots of Eq. (7) become complex, it can also lead to the occurrence of the stopband or forbidden gap (Rubia et al. 2018).

Moreover, the value (positive or negative) of the third derivative of the Sagdeev potential at $\phi = 0$ determines the polarity (positive or negative) of the nonlinear solitary structures (Verheest et al. 2006) and is given by

$$\frac{d^3 S(\phi, M)}{d\phi^3}|_{\phi=0} = f'(M_0)$$

$$\equiv \sum_j \frac{3Z_j^3 n_{j0}\left((M_0 - v_{dj})^2 + \delta_j\right)}{\mu_j^2\left((M_0 - v_{dj})^2 - 3\delta_j\right)^3}. \tag{8}$$

3 Numerical results

In the magnetosheath side of the ion diffusion region, MMS (Ergun et al. 2016) recorded the presence of cold magnetospheric plasma and warm magnetosheath plasma. Figure 1 show the existence domain for the electrostatic solitary wave structures corresponding to the electron acoustic mode as a function of equilibrium cold magnetosphere electron number density n_{c0}. The fixed plasma parameters are, warm electron drift velocity $v_{dw} = 0$, mass ratio $m_e/m_i = 1/1836$, cold electron temperature $T_c = 0.5$ eV, warm electron and ion temperature $T_w = T_i = 100$ eV, and total electron density $N_0 = 30.2$ cm^{-3} which correspond to the data set in Fig. 3(f) of Ergun et al. (2016). It is seen that there are four distinct regions in the four panels of Fig. 1, namely, negative potential solitons region (R1), negative solitons and double layers region (R2), stopband or forbidden gap region (R3) and positive potential solitons and double layers region (R4). For the case of the first (R1) region in panels $a-d$, only negative potential (rarefactive) soliton solutions are found with an upper limit of Mach number, (M_{max}), determined by the cold electron density becoming unreal. In the second (R2) region, negative potential (rarefactive) solitons are found to exist with the upper Mach number values determined by the formation of a double layer, represented by M_{DL}. The third (R3) region have no soliton or double layer solutions and are forbidden regions. The existence of nonlinear structures is discontinuous over the range in n_{c0} as solitons/double layers are not supported in an intermediate range of values of R3 regions. Beyond the forbidden region, the solitary wave polarity switched for the existence of compressive (positive potential) solitons with upper M-value determined by the formation of a double layer, M_{DL}, in the last (R4) regions. In Fig. 1(a), the cold electron drift velocity $v_{dc} = 0$ gives the existence range of R1 (n_{c0}: 0.100 – 0.299), R2 (n_{c0}: 0.300 – 0.427), R3 (n_{c0}: 0.428 – 0.430), and R4 (n_{c0}: 0.431 – 0.500). Figure 1(b) $v_{dc} = 6.50$, R1 (n_{c0}: 0.100 – 0.249), R2 (n_{c0}: 0.250 – 0.395), R3 (n_{c0}: 0.396 – 0.404), and R4 (n_{c0}: 0.405 – 0.500). For $v_{dc} = 10.0$ in Fig. 1(c), R1 (n_{c0}: 0.100 – 0.249), R2 (n_{c0}: 0.250 – 0.382), R3 (n_{c0}: 0.383 – 0.391), and R4 (n_{c0}: 0.392 – 0.500). In Fig. 1(d) $v_{dc} = 20.0$ gives, R1 (n_{c0}: 0.100 – 0.249), R2 (n_{c0}: 0.250 – 0.333), R3 (n_{c0}: 0.334 – 0.344), and R4 (n_{c0}: 0.345 – 0.500). From Fig. 1, it is clear that the existence domains R1, R2, R3 and R4 get shifted towards higher Mach numbers and lower values of the cold electron density whereas the forbidden region R3 gets wider when the cold electron drift velocity, v_{dc} is increased. Further, existence domains R1, R2 and R4 narrows down with increase in cold electron drift velocity and diminishing in cold electron number density.

For illustrations, a typical profile of the Sagdeev potential $S(\phi, M)$ against normalized electrostatic potential ϕ for the fixed plasma parameters of Fig. 1(c) for $n_{c0} = 0.15$ and $n_{w0} = 0.85$ in Region 1 (R1) is shown in Fig. 2, with the corresponding rarefactive (negative potential) solitons shown in Fig. 2(b) and the bipolar parallel electric field profiles in Fig. 2(c). Figure 3(a) represents the Sagdeev potential in R2 for $n_{c0} = 0.35$ and $n_{w0} = 0.65$, with the corresponding rarefactive (negative potential) solitons shown in Fig. 3(b). It is important to mention the existence of a double layer which forms the upper boundary of the Mach number range M_{DL} for the existence of soliton structures. Region R3 is a stopband region with no soliton/double layer solutions. Finally, Fig. 4(a) represents the Sagdeev potential in R4 for $n_{c0} = 0.4$ and $n_{w0} = 0.6$, with the corresponding compressive (positive potential) soliton structures with an upper boundary limited by a double layer formation as shown in Fig. 4(b). Properties of electron acoustic solitons and double layers corresponding to data of Fig. 1(a), (b) and (d) are similar to that of Fig. 1(c) and not shown to preserve space.

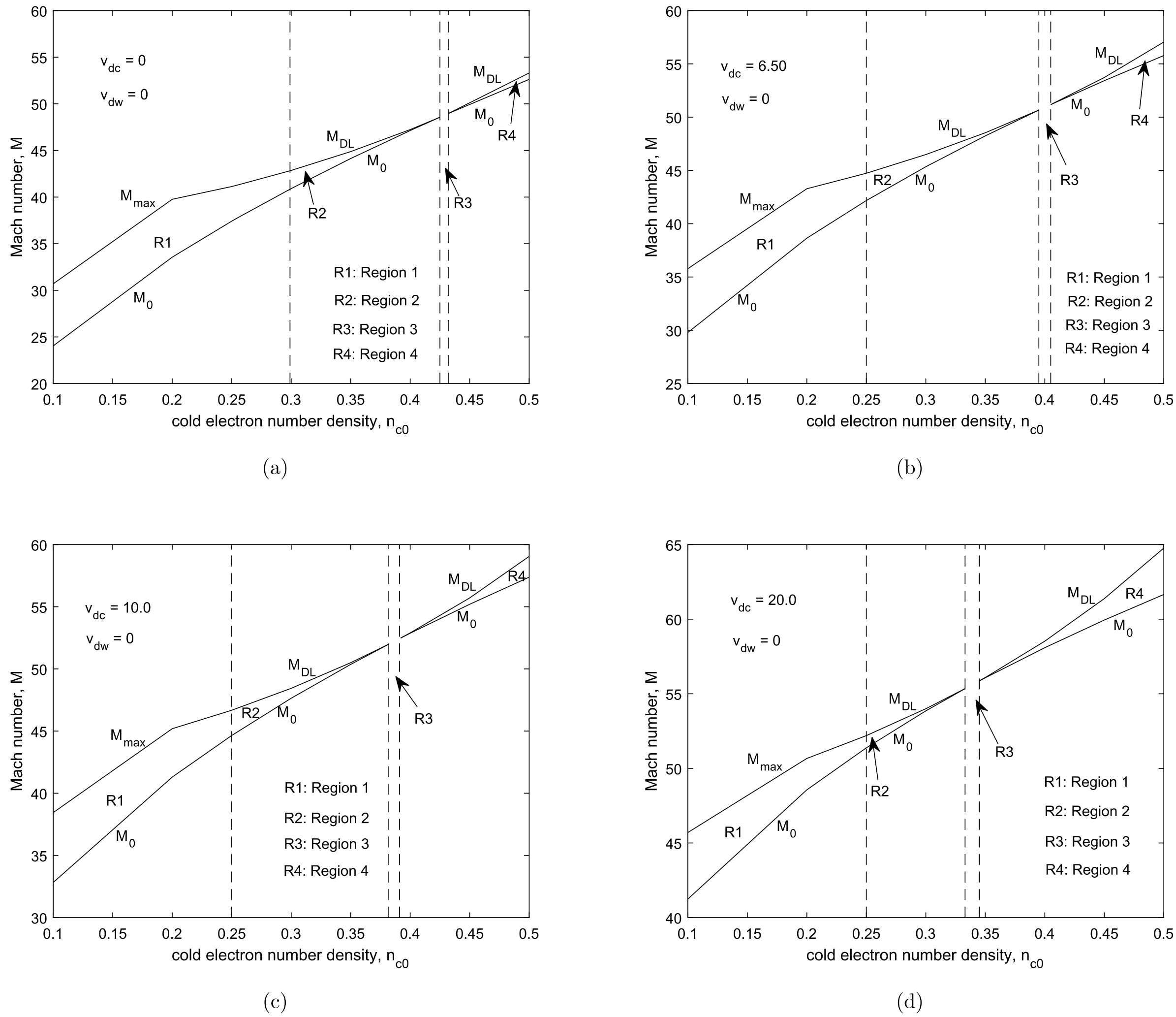

Fig. 1 Electron acoustic mode existence domain such as negative potential solitons region, negative solitons and double layers region, singularities region and positive potential solitons and double layers region for electrostatic solitary waves. The fixed plasma parameters are, $v_{dw} = 0$, $m_e/m_i = 1/1836$, $T_c = 0.5$ eV, $T_w = T_i = 100$ eV. (a) $v_{dc} = 0.0$; (b) $v_{dc} = 6.50$; (c) $v_{dc} = 10.0$; (d) $v_{dc} = 20.0$

4 Discussion and conclusions

We have studied the large-amplitude electron-acoustic solitons and double layers in an unmagnetized magnetosheath plasma consisting of cold MSP electron beam, warm magnetosheath electrons and ions. The model predicts positive and negative potential electrostatic solitons and double layers, and stopbands or forbidden gap regions in the magnetosheath side of the ion diffusion region of the Earth's magnetopause. An increase in the cold electron drift velocity, v_{dc}, leads to a wider stopband/forbidden gap (R3) region.

For the plasma parameters observed by MMS satellite (Ergun et al. 2016) in the magnetosheath, we present in Table 1 the properties of nonlinear electrostatic structures, as a function of plasma parameters, such as the electric field amplitude, width, velocities, and time duration.

Table 1 illustrates the characteristics of electron-acoustic solitons and double layers in the magnetosheath side of the ion diffusion region in terms of unnormalized electric field amplitude, E, velocities, V, width, W, and time duration, $\tau = W/V$ as a function of cold electron number density, n_{c0} respectively.

The nonlinear electrostatic structures can generate parallel electric field amplitude in the range of (0.26 – 407) mV/m. From Table 1, for $n_{c0} = 0.1 - 0.2$, we observed a negative potential solitons only representing R1 in Fig. 1(c), the electric field amplitude, soliton width, wave velocities and time duration increase with n_{c0}. For $n_{c0} = 0.3$ representing R2 in Fig. 1(c), negative potential solitons limited by the formation of double layer as an upper bound is observed and there is a slight drop in the maximum electric field amplitude due to the double layer formation. Positive potential solitons with the upper bound limited by double

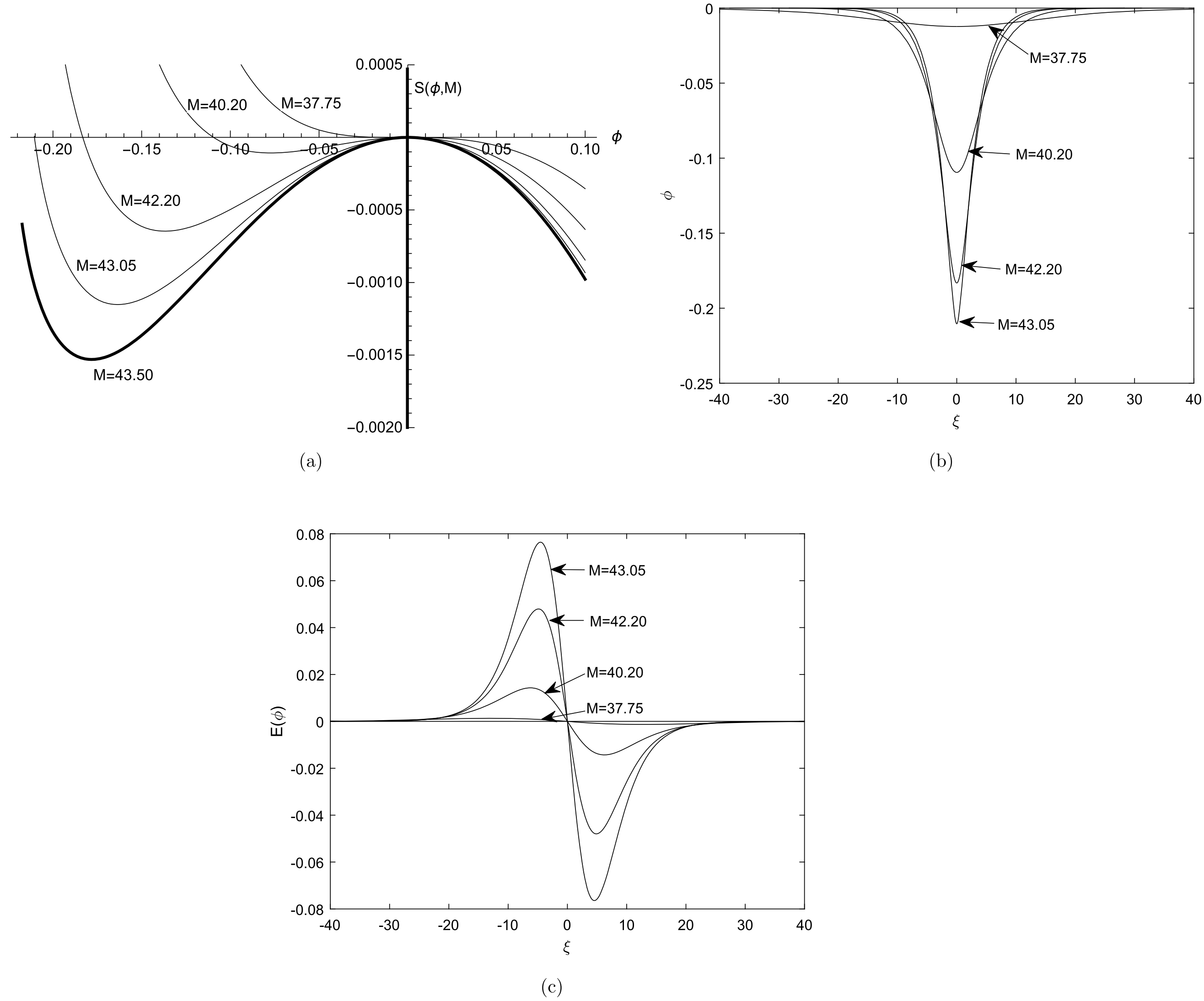

Fig. 2 Typical characteristics of R1 solitons. (a) Sagdeev potential profiles for the cold electron drift velocity $v_{dc} = 10.0$ and $n_{c0} = 0.15$, other fixed plasma parameters are $n_{w0} = 0.85$, $v_{dw} = 0$, $m_e/m_i = 1/1836$, $T_c = 0.5$ eV, $T_w = T_i = 100$ eV; (b) the corresponding rarefactive electrostatic solitons; (c) corresponding bipolar parallel electric field structures

layer were obtained in R4 for $n_{c0} = 0.4 - 0.5$, the electric field amplitude and wave velocity increase, but the soliton width and time duration decreasing. The region corresponding to $0.383 < n_{c0} < 0.391$ is the forbidden region (R3), and no solitons can exist in this region for the parameters of Table 1.

The effect of the cold electron drift velocity on the properties of the nonlinear electrostatic structures are presented in Table 2. For the fixed magnetosheath plasma parameters as in Fig. 1 and for the cold electron number density $n_{c0} = 0.25$ representing region R1 for $v_{dc} = 0$ (ref. Figure 1(a)) and Region 2 (R2) for $v_{dc} = 6.50$, 10.0 and 20.0 (ref. Figure 1(b), (c) and (d)). Electron-acoustic soliton/double layer velocity and the minimum electric field amplitude increase with the increase in the cold electron drift velocity, v_{dc}. The solitons/DLs width, pulse duration and the maximum electric field amplitude decrease by an increase in the cold electron drift velocity, v_{dc}.

Related to the spacecraft observations, Magnetospheric Multiscale (MMS) mission has reported the observations of large parallel electric field structures with amplitude on the order of 100 mV/m associated with magnetic reconnection at the magnetopause (Ergun et al. 2016) of the Earth's magnetosphere. The present theoretical study is applied to examine the characteristics of the large-amplitude broadband electrostatic solitary waves observed by the MMS in terms of nonlinear electron-acoustic solitons and double layers (DLs). For our typical computational plasma parameters, the amplitudes of the electric fields associated with electron-acoustic solitons/DLs fall in the range of (0.26-407) mV/m

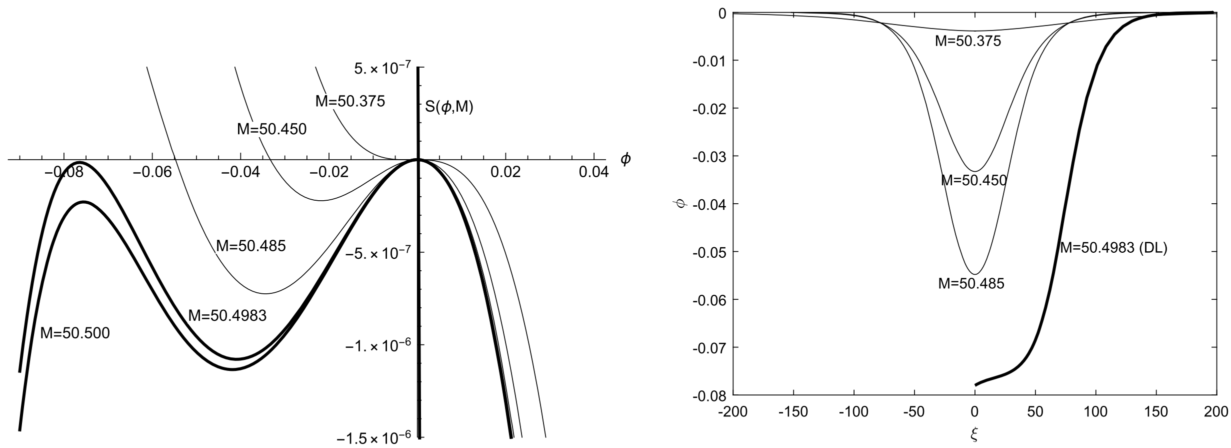

(a) (b)

Fig. 3 Typical characteristics of R2 solitons and double layers. (a) Sagdeev potential profiles for the cold electron drift velocity $v_{dc} = 10.0$ and $n_{c0} = 0.35$, other fixed plasma parameters are $n_{w0} = 0.65$, $v_{dw} = 0$, $m_e/m_i = 1/1836$, $T_c = 0.5$ eV, $T_w = T_i = 100$ eV; (b) the corresponding rarefactive electrostatic solitons and double layers

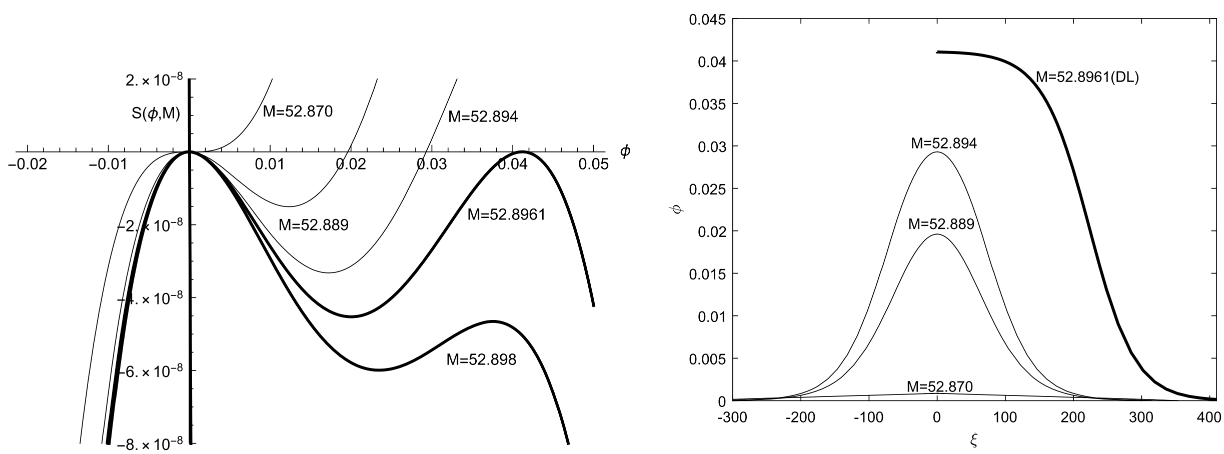

(a) (b)

Fig. 4 Typical characteristics of R4 solitons and double layers. (a) Sagdeev potential profiles for the cold electron drift velocity $v_{dc} = 10.0$ and $n_{c0} = 0.4$, other fixed plasma parameters are $n_{w0} = 0.60$, $v_{dw} = 0$, $m_e/m_i = 1/1836$, $T_c = 0.5$ eV, $T_w = T_i = 100$ eV; (b) the corresponding compressive electrostatic solitons and double layers

Table 1 Properties of electron-acoustic solitons (S) and double layers (DL) such as the velocity (V), electric field (E), width (W) and pulse duration (τ) in the magnetosheath side of the diffusion region as functions of the cold electron density n_{c0}, for $v_{dc} = 10.0$, $v_{dw} = 0.0$, $m_e/m_i = 1/1836$, $T_c = 0.5$, $T_w = T_i = 100$ eV. The corresponding magnetosphere total electron density, $N_0 = 30.2\ cm^{-3}$ (Ergun et al. 2016) yields Debye length, $\lambda_{di} = 13.5$ m

n_{c0}	polarity	$V(10^2 kms^{-1})$	$E(mVm^{-1})$	$W(m)$	$\tau(ms)$
0.1	$-ve(S)$	31.70 – 36.90	1.58 – 360	571 – 74	0.18 – 0.02
0.2	$-ve(S)$	39.70 – 43.40	1.30 – 407	813 – 103	0.20 – 0.024
0.3	$-ve(S/DL)$	45.80 – 46.50	1.00 – 110	1188 – 257	0.26 – 0.06
0.4	$+ve(S/DL)$	50.76 – 50.78	0.26 – 2.30	3321 – 3308	0.65 – 0.651
0.5	$+ve(S/DL)$	55.15 – 56.70	1.30 – 177	923 – 479	0.17 – 0.08

Table 2 Properties of electron-acoustic solitons (S) and double layers (DL) such as the velocity (V), electric field (E), width (W) and pulse duration (τ) in the magnetosheath side of the diffusion region as functions of the cold electron drift velocity v_{dc}, for $v_{dw} = 0.0$, $n_{c0} = 0.25$, $n_{w0} = 0.75$, $m_e/m_i = 1/1836$, $T_c = 0.5$, $T_w = T_i = 100$ eV. The corresponding magnetosphere total electron density, $N_0 = 30.2\ cm^{-3}$ (Ergun et al. 2016) yields Debye length, $\lambda_{di} = 13.5$ m

v_{dc}	polarity	$V(10^2 kms^{-1})$	$E(mVm^{-1})$	$W(m)$	$\tau(ms)$
0.00	$-ve(S)$	36.00 – 39.50	0.30 – 381	1606 – 143	0.45 – 0.036
6.50	$-ve(S/DL)$	40.50 – 43.00	0.51 – 377	1283 – 114	0.32 – 0.027
10.00	$-ve(S/DL)$	43.00 – 44.80	0.66 – 362	1156 – 103	0.27 – 0.023
20.00	$-ve(S/DL)$	49.40 – 50.10	0.80 – 130	1031 – 166	0.21 – 0.033

(cf. Table 1) which are in good agreement with the electrostatic waves having amplitudes of 100s mV/m observed by the MMS (Ergun et al. 2016). The fast Fourier transform (FFT) of the predicted electron-acoustic solitons/DLs would produce broadband electrostatic waves having peak frequencies near the inverse of pulse duration. Using the maximum value of the pulse durations (cf. Table 1), the peak frequencies of the broadband electrostatic waves would fall in the range of (1.5–5.8) kHz which is in fair agreement with the MMS observations of large amplitude electrostatic waves in frequency range of ~ 3.2 kHz. The existence of the stop-band/forbidden gap region can be checked by performing the data analysis for parametric space shown in R3 region of Fig. 1. This is beyond the scope of the paper.

Acknowledgements GSL thanks the Indian National Science Academy, New Delhi for the support under the INSA-Honorary Scientist Scheme. Data is available through Ergun et al Ergun et al. (2016).

Author contributions All authors contributed equally and reviewed the manuscript.

Data Availability MMS data are also open to the public. (https://lasp.colorado.edu/mms/sdc/public/).

Declarations

Competing interests The authors declare no competing interests.

References

Argall, M.R., Paulson, K., Alm, L., Rager, A., Dorelli, J., Shuster, J., Wang, S., Torbert, R.B., Vaith, H., Dors, I., Chutter, M., Farrugia, C., Burch, J., Pollock, C., Giles, B., et al.: Electron dynamics within the electron diffusion region of asymmetric reconnection. J. Geophys. Res. Space Phys. **123**, 146–162 (2018). https://doi.org/10.1002/2017JA024524

Bernstein, I.B., Greene, J.M., Kruskal, M.D.: Exact nonlinear plasma oscillations. Phys. Rev. **108**, 546 (1957). https://doi.org/10.1103/PhysRev.108.546

Berthomier, M., Pottelette, R., Malingre, M.: Solitary waves and weak double layers in a two-electron temperature auroral plasma. J. Geophys. Res. **103**(A3), 4261–4270 (1998). https://doi.org/10.1029/97JA00338

Bharuthram, R., Rufai, O.R., Maharaj, S.K.: Theoretical studies of low and high frequency electrostatic solitary waves in the magnetopause associated with asymmetric magnetic reconnection. Adv. Space Res. **69**, 3008–3018 (2022). https://doi.org/10.1016/j.asr.2022.01.034

Bostrom, R., Holback, B., Holmgren, G.: Solitary structures in the magnetospheric plasma observed by Viking. Phys. Scr. **39**, 782–786 (1989). https://doi.org/10.1088/0031-8949/39/6/022/pdf

Bulanov, S.V., Esirkepov, T.Zh., Kando, M., Koga, J.K., Pirozhkov, A.S., Nakamura, T., Bulanov, S.S., Schroeder, C.B., Esarey, E., Califano, F., Pegoraro, F.: On the breaking of a plasma wave in a thermal plasma. I. The structure of the density singularity. Phys. Plasmas **19**, 113102 (2012a). https://doi.org/10.1063/1.4764052

Bulanov, S.V., Esirkepov, T.Zh., Kando, M., Koga, J.K., Pirozhkov, A.S., Nakamura, T., Bulanov, S.S., Schroeder, C.B., Esarey, E., Califano, F., Pegoraro, F.: On the breaking of a plasma wave in a thermal plasma. II. Electromagnetic wave interaction with the breaking plasma wave. Phys. Plasmas **19**, 113103 (2012b). https://doi.org/10.1063/1.4764056

Dillard, C.S., Vasko, I.Y., Mozer, F.S., Agapitor, O.V., Bonnell, J.W.: Electron-acoustic solitary waves in the Earth inner magnetosphere. Phys. Plasmas **25**, 022905 (2018). https://doi.org/10.1063/1.5007907

Ergun, R.E., Carlson, C.W., McFadden, J.P., Mozer, F.S., Delory, G.T., Peria, W., Chaston, C.C., Temerin, M., Roth, I., Muschietti, L., Elphic, R., Strangeway, R., Pfaff, R., Cattel, C.A., Klumpar, D., Shelley, E., Peterson, W., Moebius, E., Kistler, L.: Fast satellite observations of electric field structures in the auroral zone. Geophys. Res. Lett. **25**, 2041 (1998). https://doi.org/10.1029/98GL00636

Ergun, R.E., Holmes, J.C., Goodrich, K.A., Wilder, F.D., Stawarz, J.E., Eriksson, S., Newman, D.L., Schwartz, S.J., Goldman, M.V., Sturner, A.P., Malaspina, D.M., Usanova, M.E., Torbert, R.B., Argall, M., et al.: Magnetospheric Multiscale observations of large-amplitude, parallel, electrostatic waves associated with magnetic reconnection at the magnetopause. Geophys. Res. Lett. **43**, 5626–5634 (2016). https://doi.org/10.1002/2016GL068992

Goodrich, K.A., Ergun, R., Schwartz, S.J., Wilson, L.B., Newman, D., Wilder, F.D., Holmes, J., Johlander, A., Burch, J., Torbert, R., Khotyaintsev, Y., Lindqvist, P., Strangeway, R., Russell, C., Gershman, D., Giles, B., Andersson, L.: MMS observations of electrostatic waves in an oblique shock crossing. J. Geophys. Res. Space Phys. **123**(11), 9430–9442 (2018). https://doi.org/10.1029/2018JA025830

Graham, D.B., Khotyaintsev, Yu.V., Vaivads, A., Andre, M.: Electrostatic solitary waves with distinct speeds associated with asymmetric reconnection. Geophys. Res. Lett. **42**, 215224 (2015). https://doi.org/10.1002/2014GL062538

Graham, D.B., Vaivads, A., Khotyaintsev, Yu.V., Andre, M., Le Contel, O., Malaspina, D.M., Lindqvist, P.-A., Ergun, R.E., Gershman, D.J., Giles, B.L., Magnes, W., Russell, C.T., Burch, J.L., Torbert, R.B.: Large-amplitude high-frequency waves at Earth's magnetopause. J. Geophys. Res. Space Phys. **123**, 2630–2657 (2018). https://doi.org/10.1002/2017JA025034

Huang, S.: The Earth's magnetosheath: structures, waves and turbulence. Rev. Geophys. Planet. Phys. **53**(5), 517–531 (2022). https://doi.org/10.19975/jdqyxx.2002-014

Hui, L., Jiang, W., Wang, C., Verscharen, D., Zeng, C., Russell, C.T., Giles, B., Burch, J.L.: Evolution of the Earth's magnetosheath turbulence: a statistical study based on MMS observations. Astrophys. J. Lett. **898**, L43 (2020). https://doi.org/10.3847/2041-8213/aba531

Hutchinson, I.H.: Electron holes in phase space: what they are and why they matter. Phys. Plasmas **24**(5), 055601 (2017). https://aip.scitation.org/doi/10.1063/1.4976854

Kakad, A.P., Singh, S.V., Reddy, R.V., Lakhina, G.S., Tagare, S.G., Verheest, F.: Generation mechanism for electron acoustic solitary waves. Phys. Plasmas **14**, 052305 (2007). https://doi.org/10.1063/1.2732176

Kakad, A., Kakad, B., Anekallu, C., Lakhina, G., Omura, Y., Fazakerley, A.: Slow electrostatic solitary waves in the Earth's plasma sheet boundary layer. J. Geophys. Res. Space Phys. **121**, 4452–4465 (2016). https://doi.org/10.1002/2016JA022365

Kamaletdinov, S.R., Hutchinson, I.H., Vasko, I.Y., Artemyev, A.V., Lotekar, A., Mozer, F.: Spacecraft observations and theoretical understanding of slow electron holes. Phys. Rev. Lett. **127**, 165101 (2021). https://doi.org/10.1103/PhysRevLett.127.165101

Lakhina, G.S., Singh, S.V., Kakad, A.P., Verheest, F., Bharuthram, R.: Study of nonlinear ion- and electron-acoustic waves in multi-component space plasmas. Nonlinear Process. Geophys. **15**, 903–913 (2008). https://doi.org/10.5194/npg-15-903-2008

Lakhina, G.S., Singh, S.V., Kakad, A.P., Goldstein, M.L., Vin˜as, A.F., Pickett, J.S.: A mechanism for electrostatic solitary structures in the Earth's magnetosheath. J. Geophys. Res. **114**, A09212 (2009). https://doi.org/10.1029/2009JA014306

Lakhina, G.S., Singh, S.V., Kakad, A.P.: Ion-and electron-acoustic solitons and double layers in multi-component space plasmas. Adv. Space Res. **47**, 1558–1567 (2011a). https://doi.org/10.1016/j.asr.2010.12.013

Lakhina, G.S., Singh, S.V., Kakad, A.P., Pickett, J.S.: Generation of electrostatic solitary waves in the plasma sheet boundary layer. J. Geophys. Res. Space Phys. **116**, A10218 (2011b). https://doi.org/10.1029/2011JAA016700

Lakhina, G.S., Singh, S.V., Rubia, R., Sreeraj, T.: A review of nonlinear fluid models for ion- and electron-acoustic solitons and double layers: application to weak double layers and electrostatic solitary waves in the solar wind and the lunar wake. Phys. Plasmas **25**, 080501 (2018). https://doi.org/10.1063/1.5033498

Lakhina, G.S., Singh, S.V., Rubia, R., Devanandhan, S.: Electrostatic solitary structures in space plasmas: soliton perspective. Plasma **4**, 681–731 (2021). https://doi.org/10.3390/plasma4040035

Lotekar, A., Kakad, A., Kakad, B.: Formation of asymmetric electron acoustic double layers in the Earth's inner magnetosphere. J. Geophys. Res. Space Phys. **124**, 6896–6905 (2019). https://doi.org/10.1029/2018JA026303

Lotekar, A., Vasko, I.Y., Mozer, F.S., Hutchinson, I., Artemyev, A.V., Bale, S.D., Bonnell, J.W., Ergun, R., Giles, B., Khotyaintsev, Yu.V., Lindqvist, P.A., Russell, C.T., Strangeway, R.: Multisatellite MMS analysis of electron holes in the Earth's magnetotail: origin, properties, velocity gap, and transverse instability. J. Geophys. Res. Space Phys. **125**, e2020JA028066 (2020). https://doi.org/10.1029/2020JA028066

Maharaj, S.K., Bharuthram, R., Singh, S.V., Lakhina, G.S.: Existence domains of arbitrary amplitude nonlinear structures in two-electron temperature space plasmas. II. High-frequency electron – acoustic solitons. Phys. Plasmas **19**, 122301 (2012a). https://doi.org/10.1063/1.4769174

Maharaj, S.K., Bharuthram, R., Singh, S.V., Lakhina, G.S.: Existence domains of arbitraryamplitude nonlinear structures in two-electron temperature space plasmas. I. Low-frequency ion- acoustic solitons. Phys. Plasmas **19**, 072320 (2012b). https://doi.org/10.1063/1.4737895

Maharaj, S.K., Bharuthram, R.: New insights of fast ion-acoustic soliton stopbands and extension to dusty plasmas. Phys. Plasmas **27**, 032306 (2020). https://doi.org/10.1063/1.5130540

Matsumoto, H., Kojima, H., Miyatake, T., Omura, Y., Okada, Y.M., Nagano, I., Tsutui, M.: Electrostatic solitary waves (ESW) in the magnetotail: Ben wave forms observed by GEOTAIL. Geophys. Res. Lett. **21**, 2915–2918 (1994). https://doi.org/10.1029/94GL01284

Mozer, F.S., Agapitov, O.V., Artemyev, A., Drake, J.F., Krasnoselskikh, V., Lejosne, S., Vasko, I.: Time domain structures: what and where they are, what they do, and how they are made. Geophys. Res. Lett. **42**, 3627–3638 (2015). https://doi.org/10.1002/2015GL063946

Mozer, F.S., Bonnell, J.W., Hanson, E.L.M., Gasque, L.C., Vasko, I.Y.: Nonlinear ion-acoustic waves, ion holes, and electron holes in the near-sun solar wind. Astrophys. J. **911**, 89 (2021). https://doi.org/10.3847/1538-4357/abed52

Muschietti, L., Ergun, R.E., Roth, I., Carlson, C.W.: Phase-space electron holes along magnetic field lines. Geophys. Res. Lett. **26**, 1093 (1999). https://doi.org/10.1029/1999GL900207

Omura, Y., Kojima, H., Matsumoto, H.: Computer simulation of electrostatic solitary waves: a nonlinear model of Broadband electrostatic noise. Geophys. Res. Lett. **21**, 2923–2926 (1994). https://doi.org/10.1029/94GL01605

Pickett, J.S., Menietti, J.D., Gurnett, D.A., Tsurutani, B., Kintner, P., Klatt, E., Balogh, A.: Solitary potential structures observed in the magnetosheath by the Cluster spacecraft. Nonlinear Process. Geophys. **10**, 3–11 (2003). https://doi.org/10.5194/npg-10-3-2003.

Pickett, J.S., Chen, L.-J., Kahler, S.W., Santolik, O., Gurnett, D.A., Tsurutani, B.T., Balogh, A.: Isolated electrostatic structures observed throughout the Cluster orbit: relationship to magnetic field strength. Ann. Geophys. **22**, 2515–2523 (2004). https://doi.org/10.5194/angeo-22-2515-2004

Pickett, J.S., Chen, L.-J., Kahler, S.W., Santolik, O., Goldstein, M.L., Lavraud, B., Decreau, P.M., Kessel, R., Lucek, E., Lakhina, G.S., Tsurutani, B.T., Gurnett, D.A., Cornilleau-Wehrlin, N., Fazakerley, A., Reme, H., Balogh, A.: On the generation of solitary waves observed by cluster in the near-Earth magnetosheath. Nonlinear Process. Geophys. **12**(2), 181–193 (2005). https://doi.org/10.5194/npg-12-181-2005

Rubia, R., Singh, S.V., Lakhina, G.S.: Existence domains of electrostatic solitary structures in the solar wind plasma. Phys. Plasmas **23**(6), 062902 (2016a). https://doi.org/10.1063/1.4953892

Rubia, R., Singh, S.V., Lakhina, G.S.: Erratum "Existence domains of electrostatic solitary structures in the solar wind plasma". Phys. Plasmas **23**, 119903 (2016b). https://doi.org/10.1063/1.4967357

Rubia, R., Singh, S.V., Lakhina, G.S.: Existence domain of electrostatic solitary waves in the lunar wake. Phys. Plasmas **25**, 032302 (2018). https://doi.org/10.1063/1.5017638

Rufai, O.R., Bharuthram, R., Singh, S.V., Lakhina, G.S.: Low frequency solitons and double layers in a magnetized plasma with two temperature electrons. Phys. Plasmas **19**, 122308 (2012). https://doi.org/10.1063/1.4771574

Rufai, O.R., Bharuthram, R., Singh, S.V., Lakhina, G.S.: Effect of hot ion temperature on obliquely propagating ion-acoustic solitons and double layers in an auroral plasma. Commun. Nonlinear Sci. Numer. Simul. **19**, 1338–1346 (2014). https://doi.org/10.1016/j.cnsns.2013.09.024

Rufai, O.R.: Auroral electrostatic solitons and supersolitons in a magnetized nonthermal plasma. Phys. Plasmas **22**, 052309 (2015). https://doi.org/10.1063/1.4921740

Rufai, O.R., Bharuthram, R.: Electrostatic fluctuations in a magnetized two-component plasma with q-nonextensive electrons and thermal ions. Phys. Plasmas **23**, 092306 (2016). https://doi.org/10.1063/1.4963773

Rufai, O.R., Bharuthram, R., Singh, S.V., Lakhina, G.S.: Obliquely propagating ion-acoustic solitons and supersolitons in four-component auroral plasmas. Adv. Space Res. **57**(3), 813–820 (2016). https://doi.org/10.1016/j.asr.2015.11.021

Rufai, O.R., Bharuthram, R.: Obliquely propagating low-frequency magnetospheric electrostatic solitary waves in the presence of an oxygen-ion beam. Commun. Nonlinear Sci. Numer. Simul. **68**, 160 (2019). https://doi.org/10.1016/j.cnsns.2018.08.006

Rufai, O.R., Khazanov, G.V., Singh, S.V.: Finite amplitude electron-acoustic waves in the electron diffusion region. Results Phys. **24**, 104041 (2021a). https://doi.org/10.1016/j.rinp.2021.104041

Rufai, O.R., Bharuthram, R., Maharaj, S.K.: The effects of superthermal particles on the existence domain of oblique low-frequency solitary waves in multi-component magnetospheric plasmas. Phys. Plasmas **28**, 052901 (2021b). https://doi.org/10.1063/5.0031330

Rufai, O.R., Khazanov, G.V., Singh, S.V., Lakhina, G.S.: Large-amplitude electrostatic fluctuations at the Earth's magnetopause with a vortex-like distribution of hot electrons. Results Phys. **35**, 105343 (2022). https://doi.org/10.1016/j.rinp.2022.105343

Sagdeev, R.Z.: In: Leontovich, M.A. (ed.) Reviews of Plasma Physics, vol. 4. Consultants Bureau, New York (1966)

Schamel, H.: Stationary solitary, snoidal and sinusoidal ion acoustic waves. Plasma Phys. **14**, 905 (1972). https://iopscience.iop.org/article/10.1088/0032-1028/14/10/002

Schamel, H.: Theory of electron holes. Phys. Scr. **20**, 336–342 (1979). https://doi.org/10.1088/0031-8949/20/3-4/006/pdf

Singh, S.V., Reddy, R.V., Lakhina, G.S.: Broadband electrostatic noise due to nonlinear electron-acoustic waves. Adv. Space Res. **28**(11), 1643–1648 (2001)

Singh, S.V., Lakhina, G.S., Bharuthram, R., Pillay, S.R.: Electrostatic solitary structures in presence of non-thermal electrons and a warm electron beam on the auroral field lines. Phys. Plasmas **18**, 122306 (2011). https://doi.org/10.1063/1.3671955

Temerin, M., Cerny, K., Lotko, W., Mozer, F.S.: Observations of double layers and solitary waves in the auroral plasma. Phys. Rev. Lett. **48**, 1175 (1982). https://doi.org/10.1103/PhysRevLett.48.1175

Tong, Y., Vasko, I., Mozer, F.S., Bale, S.D., Roth, I., Artemyev, A.V., Ergun, R., Giles, B., Lindqvist, P.-A., Russell, C.T., Strangeway, R., Torbert, R.B.: Simultaneous multispacecraft probing of electron phase space holes. Geophys. Res. Lett. **45**, 11513–11519 (2018). https://doi.org/10.1029/2018GL079044

Tsurutani, B.T., Arballo, J.K., Lakhina, G.S., Ho, C.M., Buti, B., Pickett, J.S., Gurnett, D.A.: Plasma waves in the dayside polar cap boundary layer: bipolar and monopolar electric pulses and whistler mode waves. Geophys. Res. Lett. **25**(22), 4117–4120 (1998). https://doi.org/10.1029/1998GL900114

Vasko, I.Y., Agapitov, O.V., Mozer, F.S., Bonnell, J.W., Artemyev, A.V., Krasnoselskikh, V.V., Reeves, G., Hospodarsky, G.: Electron-acoustic solitons and double-layers in the inner magnetosphere. Geophys. Res. Lett. **44**, 4575–4583 (2017). https://doi.org/10.1002/2017GL074026

Vasko, I.Y., Agapitov, O.V., Mozer, F.S., Bonnell, J.W., Artemyev, A.V., Krasnoselskikh, V.V., Tong, Y.: Electrostatic steepening of whistler waves. Phys. Rev. Lett. **120**, 195101 (2018). https://doi.org/10.1103/PhysRevLett.120.195101

Vasko, I.Y., Wang, R., Mozer, F.S., Bale, S.D., Artemyev, A.V.: On the nature and origin of bipolar electrostatic structures in the Earth's bow shock. Front. Phys. **8**, 156 (2020). https://doi.org/10.3389/fphy.2020.00156

Verheest, F., Cattaert, T., Hellberg, M.A., Mace, R.L.: On the existence of ion-acoustic double layers in two-electron temperature plasmas. Phys. Plasmas **13**, 042301 (2006). https://doi.org/10.1063/1.2187448

Verheest, F., Hellberg, M.A.: Stopbands in fast ion-acoustic soliton propagation revisited. Phys. Plasmas **27**, 102306 (2020). https://doi.org/10.1063/5.0021956

Wang, R., Vasko, I.Y., Mozer, F.S., Bale, S.D., Kuzichev, I.V., Artemyev, A.V., Steinvall, K., Ergun, R., Giles, B., Khotyaintsev, Y., Lindqvist, P.-A., Russell, C.T., Strangeway, R.: Electrostatic solitary waves in the Earth's bow shock: nature, properties, lifetimes, and origin. J. Geophys. Res. Space Phys. **126**, 7 (2021). https://doi.org/10.1029/2021JA029357